COMPUTERS &
GEOSCIENCES
AN INTERNATIONAL JOURNAL

EDITOR-IN-CHIEF
JEF CAERS
STANFORD UNIVERSITY

Contents lists available at ScienceDirect

Computers & Geosciences

journal homepage: www.elsevier.com/locate/cageo

CrossMark
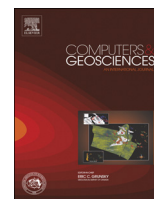
psd: Adaptive, sine multitaper power spectral density estimation for R

Andrew J. Barbour *, Robert L. Parker

Institute of Geophysics and Planetary Physics, Scripps Institution of Oceanography, University of California, San Diego, 9500 Gilman Dr. La Jolla, CA 92093-0225, United States

ARTICLE INFO

ABSTRACT

We present an R package for computing univariate power spectral density estimates with little or no tuning effort. We employ sine multitapers, allowing the number to vary with frequency in order to reduce mean square error, the sum of squared bias and variance, at each point. The approximate criterion of Riedel and Sidorenko (1995) is modified to prevent runaway averaging that otherwise occurs when the curvature of the spectrum goes to zero. An iterative procedure refines the number of tapers employed at each frequency. The resultant power spectra possess significantly lower variances than those of traditional, non-adaptive estimators. The sine tapers also provide useful spectral leakage suppression. Resolution and uncertainty can be estimated from the number of degrees of freedom (twice the number of tapers).

This technique is particularly suited to long time series, because it demands only one numerical Fourier transform, and requires no costly additional computation of taper functions, like the Slepian functions. It also avoids the degradation of the low-frequency performance associated with record segmentation in Welch's method. Above all, the adaptive process relieves the user of the need to set a tuning parameter, such as time-bandwidth product or segment length, that fixes frequency resolution for the entire frequency interval; instead it provides frequency-dependent spectral resolution tailored to the shape of the spectrum itself.

We demonstrate the method by applying it to continuous borehole strainmeter data from a station in the Plate Boundary Observatory, namely station B084 at the Piñon Flat Observatory in southern California. The example illustrates how psd elegantly handles spectra with large dynamic range and mixed-bandwidth features—features typically found in geophysical datasets.

1. Introduction

Power spectra play an important role in every branch of geophysics where time series are encountered. By decomposing complex signals into their frequency components, one can usually separate out phenomena according to their physical causes, or distinguish geophysically significant signals from instrumental noise. The process by which power spectra or, more precisely, power spectral densities are estimated from a discretely sampled series has, of course, evolved over many decades. Papers discussing spectral analysis in some form number in the thousands, and we make no attempt to review them here. However, we can point to a few landmark studies which have addressed the issues of both bias (from spectral leakage and curvature) and variance in a profound way: Welch (1967), Thomson (1982), and Riedel and Sidorenko (1995). As we will see all of these appeal to the idea of multitapers.

Geophysical time series often exhibit very large dynamic ranges, great record lengths, and a mixture of wide and narrow-band processes. An effective computer program must be able to handle these issues efficiently and, in our view, should not require the user to experiment repeatedly with parameter settings in order to obtain a satisfactory spectrum. The sine-multitaper approach of Riedel and Sidorenko (1995) meets our requirements best: it is adaptive, so that the resolution and variance are set by the spectral shape, not the user; it is fast, requiring only one numerical Fourier transform for the whole analysis; bias and variance are kept in balance at every frequency.

The plan of the paper is as follows: we give a brief outline of the theory, summarizing the results of Riedel and Sidorenko (1995) and describing our modest contribution. Then we describe the implementation as a program, and conclude with an illustration from a fairly typical geophysical record.

2. Power spectral density estimation

The standard method of decomposition of a record by frequency is to estimate the power spectral density (PSD) of the series. For a stationary stochastic signal $x(t)$ (the ideal statistical entity on which the theory is predicated), the PSD $S_x(f)$ gives the variance per unit bandwidth; essentially $S_x(f)df$ is the energy level of the signal after it has been passed through a perfect narrow

band-pass filter centered on f with width df. Our task is to make an estimate from a uniformly sampled, finite-length sample of $x(t)$, the only kind realistically available. The 'raw periodogram' is obtained from the digital Fourier transform of the finite record, and is in fact the basis for all the so-called 'direct' estimation procedures:

$$\hat{S}_x(k\Delta f) = \frac{1}{T}\left|\sum_{j=0}^{N-1} x_j \exp\frac{2\pi ijk}{N}\right|^2, \quad k = 0, 1, 2, \ldots, N/2 \tag{1}$$

where T is the record length of the N samples x_j and $\Delta f = 1/T$. It is well known (see, for example, Percival and Walden, 1993) that these estimates of $S_x(k\Delta f)$ are very unsatisfactory: they suffer from very large variances yielding uncertainties as large as the estimates themselves, and from a kind of bias, spectral leakage, where energy at one frequency spills into neighboring frequencies.

An established technique to reduce spectral leakage is to 'taper' the record, which means multiplying $x(t)$ by a carefully chosen function $\phi(t)$, the taper, before taking the numerical Fourier transform. The result is a spectrum that is the convolution of the periodogram with $|\Phi(f)|^2$, where $\Phi(f)$ is the Fourier transform of ϕ. The literature is replete with recipes for good tapers, but it is now generally recognized that the prolate spheroidal functions introduced by Slepian (1961) provide optimal suppression of leakage; see also Thomson (1982). These tapers, while not eliminating the bias completely, do a remarkably good job.

But tapering the series does nothing to reduce the variance of the periodogram estimate; for that we need some sort of averaging scheme. A popular approach is Welch's method (Welch, 1967), which briefly goes as follows: the record is broken into M equal-length, tapered segments; a periodogram is then calculated for each segment, and the final spectrum is the mean of the M periodograms. Although this method does address the issues of bias and variance together, it is unsatisfactory for several reasons. First, because the effective record is shortened by a factor of M, there is a severe loss of low frequency resolution, particularly when a lot of averaging is needed. Second, there is no good theory for choosing M, the number of segments; this parameter sets an inherent tradeoff between resolution and variance reduction for the whole spectrum. Third, the variance reduction and resolution are fixed for all frequencies.

Another approach for reducing variance is to smooth the tapered periodogram. The success of any smoothing procedure depends strongly on the choice of smoothing kernel. For example, using a relatively wide kernel will improve higher-frequency features, but will tend to degrade and actually distort lower-frequency spectra. Furthermore, neighboring spectral estimates after tapering are not statistically independent, reducing the efficiency of variance reduction produced by smoothing. We note that the non-parametric spectrum-estimation tool in R, `stats::spec.pgram`, can apply a single taper to the series, form a periodogram, and then (optionally) apply a smoothing kernel (Cowpertwait and Metcalfe, 2009).

A more satisfactory technique to reduce both spectral bias and variance is the multitaper method. Percival and Walden (1993) provide an accessible account of the topic, which was initiated by the seminal work of Thomson (1982). Thomson showed that, for a series of length T, tapering with an orthogonal set of functions ϕ_k satisfying

$$\int_0^T \prod_{k=1}^M \phi_k(t)\, dt = 0 \tag{2}$$

results in a set of statistically independent periodograms which may be averaged. This is the basis of multitaper spectral analysis.

Welch's method is an example. If non-overlapping sections are chosen and the taper for each segment is the function $\phi_0(t)$, we combine this with normalized boxcar functions $\sqcap_k$ centered at t_k; then the set of multitapers is $\phi_k(t) = \phi_0(t) \cdot \sqcap_k(t), k = 1, 2, 3 \ldots, M$. The functions $\phi_k(t)$ are orthogonal and they satisfy Eq. (2). Although this form of Welch's method qualifies as a multitaper analysis, its results are none-the-less plagued with the limitations previously mentioned. Far better performance can be achieved with different choices of ϕ_k.

The poor low-frequency behavior of Welch's method is completely eliminated in the following scheme. Thomson (1982) proposes the discrete prolate spheroidal (or Slepian) sequences as the family of orthogonal tapers; these functions are constructed to exhibit maximal leakage rejection. Unlike the Welch tapers, which vanish on a large fraction of the time interval, each function oscillates throughout the whole record. Once the frequency resolution parameter, the time-bandwidth product, has been set, the number of tapers needed to achieve the best variance can be calculated. The problem of leakage having been effectively dealt with, another form of bias becomes more serious: tapered periodograms are affected by curvature bias, a local effect that tends to flatten peaks in the spectrum. Peaks in Slepian-tapered spectra take on a characteristic 'boxy' shape. Though not widely known, there is a cure for the problem; see Prieto et al. (2007). None-the-less, the Slepian-tapered spectra suffer from two drawbacks. First, the user still must decide on a single parameter (the time-bandwidth product) that sets the resolution and variance reduction everywhere in the spectrum. Second, for very long records, the calculations of the multiple Fourier transforms and of the tapers themselves become expensive, particularly when heavy variance reduction (averaging periodograms) is required. Both these questions are addressed by the next family of tapers.

Riedel and Sidorenko (1995) consider the question of curvature bias described in the previous paragraph. By solving the appropriate optimization they find tapers that minimize a measure of the curvature bias, and furthermore, demonstrate that the family is well approximated by a set of simple sine functions:

$$\phi_k(t) = \sqrt{\frac{2}{T}}\, \sin\, \frac{k\pi t}{T}, \quad 0 \le t \le T, \ k = 1, 2, 3, \ldots \tag{3}$$

Next they tackle the question of how many tapers should be used by examining the mean square error (MSE) at each frequency. The MSE is the sum of the squared bias, β^2, and the variance, $\mathcal{V}$, the two quantities that degrade spectral estimates. They find an approximation for MSE

$$L = \beta^2 + \mathcal{V}\left\{\hat{S}(f)\right\} = \frac{S''(f)^2 K^4}{576 T^4} + \frac{S(f)^2}{K} \tag{4}$$

where K is the number of tapered periodograms averaged, and $S''(f)$ is the second derivative of the PSD with frequency. A simple differentiation yields the following expression for the value associated with the smallest possible MSE:

$$K_{\text{opt}}(f) = \left(\frac{12 T^2 S(f)}{|S''(f)|}\right)^{2/5} = 2.70192\left(\frac{T^2 S(f)}{|S''(f)|}\right)^{2/5} \tag{5}$$

Application of this formula completely avoids the difficulty of having to choose some overall balance between resolution and variance applicable to the whole spectrum: Eq. (5) does this automatically at each frequency. It means spectra with a mixture of narrow-band and wide-band features present no difficulty. This is called 'adaptive' estimation because the estimator adapts the balance of resolution and variance to the local shape of the spectrum.

Remarkably, the sine multitapers also dispose of another drawback mentioned earlier, computational expense for very long records. As Riedel and Sidorenko casually remark, there is no need to perform more than one (double length) numerical Fourier

transform for the whole record. Multiplying the signal by a sine function like those in Eq. (3) merely causes frequency shifts in the transform; all the information needed to find the transform of any tapered record is available after one FFT.

The sine multitapers are designed to minimize curvature bias; what about spectral leakage? The tapers in Eq. (3) offer a moderate amount of leakage protection (see the next section), but far less than the Slepian functions. Here again the advantage tilts to sine multitapers for long records: at any fixed frequency the error from spectral leakages tends to zero as the record length increases, since periodograms are asymptotically unbiased.

Finally, we must mention a paradox inherent in Eq. (5): to find K_{opt} one apparently needs to know the spectrum and its second derivative. There is no analytic solution to the problem of simultaneously finding K_{opt} and S and so one must resort to an iterative procedure. Starting from a pilot estimate of the spectrum, which provides preliminary values for the number of tapers, one makes another estimate; this yields values for K_{opt}, which are employed to estimate a new spectrum, and so on. This naive approach fails because Eq. (5) is an approximation with a fatal flaw: when the second derivative $S''(f)$ vanishes, the expression demands infinitely many tapers. Very small values of $|S''|$, if not exact zeros, arise in almost every real spectrum, and so this is a serious matter. The consequent runaway averaging must be suppressed: we have adopted an *ad hoc* procedure, which will be described in Section 4.

3. Further properties of sine multitapers

The effect in the frequency domain of tapering the record with the function $\phi(t)$ is to convolve the corresponding periodogram with a function closely approximated by the squared Fourier transform $|\Phi(f)|^2$; see Percival and Walden (1993). The convolution broadens spectral peaks, but also reduces the energy that would otherwise spill out of the peak into neighboring frequencies, thus curtailing the bias called spectral leakage. For the sine tapers in Eq. (3) this gives

$$|\Phi_k(f)|^2 = \frac{2Tk^2}{(k+2Tf)^2}\, \text{sinc}(Tf - k/2)^2 \qquad (6)$$

These functions, which we will call spectral kernels, are illustrated in Fig. 1. We see that the width of the central portion is roughly $k\Delta f$ and, from Eq. (6), outside that region $|\Phi_k(f)|^2$ dies away as f^{-4}.

The convolved periodograms must be averaged to obtain the multitaper estimate. In principle each periodogram is providing an estimate of the same function S, but those associated with higher k
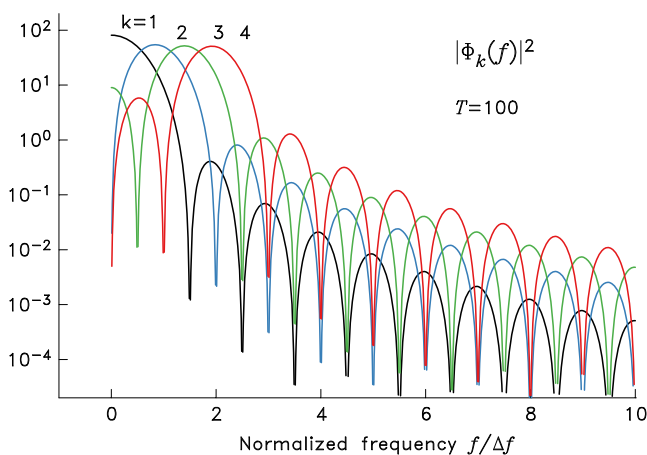
are relying more heavily on spectral values further from the central frequency. For this reason Riedel and Sidorenko suggest a parabolic weighting scheme that gives less weight to the outer

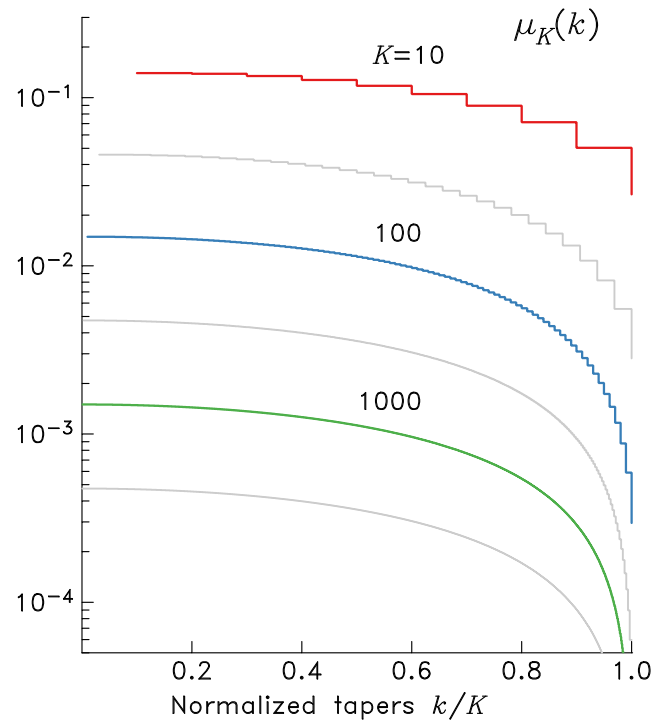**Fig. 2.** Spectral weighting factors given by Eq. (7) for selected taper sequences. These curves are quantized depending on the length of the taper sequence.

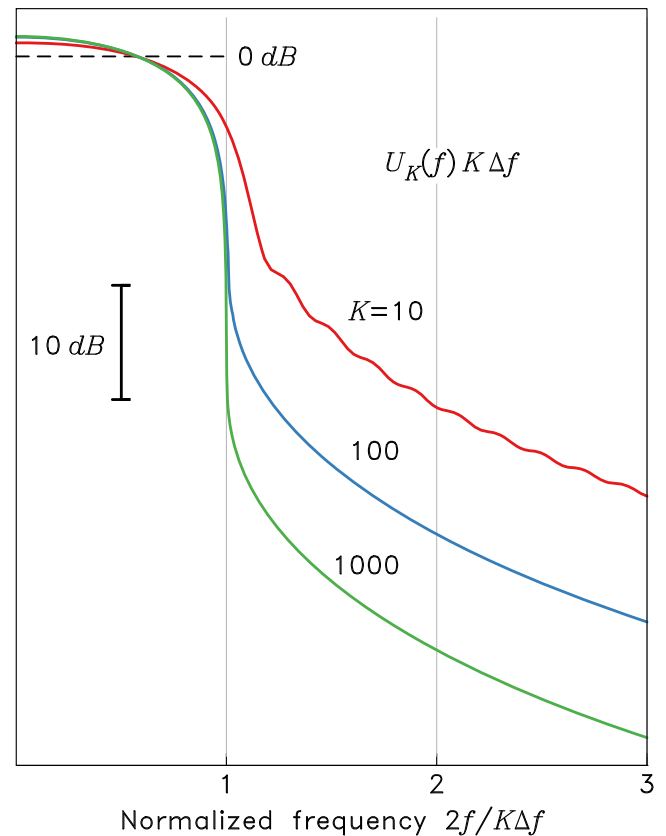

Fig. 3. Effective spectral kernels given by Eq. (9). Only the right side is shown of these symmetric functions.

Fig. 1. Spectral kernels given in Eq. (6). These functions are symmetrical about $f=0$; only the right side is shown.

members:

$$\hat{S}_x(f) = \sum_{k=1}^{K} N_k^{-1}[K^2 - (k-1)^2]\hat{S}_k(f) = \sum_{k=1}^{K} \mu_k \hat{S}_k(f) \qquad (7)$$

where $\hat{S}_k(f)$ is the periodogram tapered with ϕ_k and $N_k = K(4K-1)(K+1)/6$. The weighting is shown in Fig. 2.

With parabolic weighting the optimal number of tapers is slightly different:

$$K_{\text{opt}} = 480^{1/5} \left(\frac{T^2 S(f)}{|S''(f)|} \right)^{2/5} = 3.43754 \left(\frac{T^2 S(f)}{|S''(f)|} \right)^{2/5} \qquad (8)$$

The effective spectral kernel for the complete sum is obtained by the weighted average

$$U_K(f) = \sum_{k=1}^{K} \mu_k |\Phi_k(f)|^2 \qquad (9)$$

and this function is illustrated in Fig. 3. As expected the width of $U_K(f)$ is $K\Delta f$, which can be identified as the spectral resolution of the estimate. Somewhat surprisingly, the fraction of energy outside the central band, the part contributing to leakage, decreases as the number of tapers grows.

Given the statistical independence of the K periodogram estimates, and the parabolic weighting, it is a short calculation to show that the variance of the final estimate is approximately

$$\mathcal{V}\left\{\hat{S}(f)\right\} = \frac{6S(f)^2}{5K} \qquad (10)$$

If the time series has a Gaussian distribution, $\hat{S}$ will be distributed as χ^2 with $2K$ degrees of freedom. One can compute confidence limits knowing this, but for most purposes the asymptotic approximation of a Gaussian distribution for $\hat{S}$ is perfectly adequate.

An important distinction between adaptive and non-adaptive PSD estimates is the far smaller variance of the former in many cases. As we will see in the final section, it is not uncommon for K to be many hundreds in regions of the spectrum where $S(f)$ is flat. Such strong averaging is essentially impossible for Welch's method, because it could lead to ridiculously short segments. This difficulty obviously does not apply to Slepian-tapered estimates, because the same amount of averaging would be applied to the whole spectrum, any narrow-band features would be completely ironed out. If an adaptive scheme is contemplated for these tapers to overcome the defect, the computational cost (hundreds of Fourier transforms per frequency) suggests it would be impractical for any but the shortest series.

4. Algorithm summary

The function pspectrum applies the sine-multitaper adaptive method to produce a PSD of the input series. A rough sketch of the
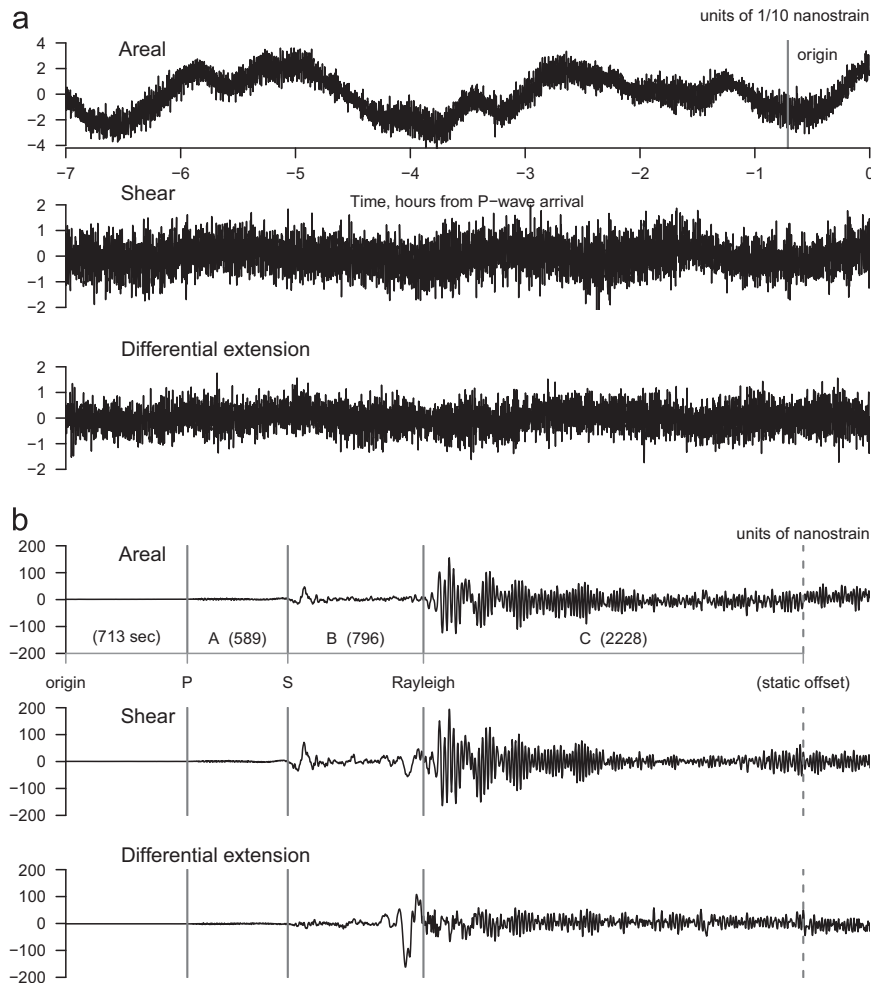

Fig. 4. Strainmeter data at PBO station B084 (a) before, and (b) after the 2011 M_w 9 Tohoku-oki earthquake (8640 km away at 307°). The sections shown in (b), labeled A–C, correspond to those in Fig. 6; section (C) ends arbitrarily at a spurious, static offset. Note the scale changes within (a), and between (a) and (b). One nanostrain is 10^{-9}, extension positive.

iterative algorithm is as follows. An initial multitaper PSD is calculated with a fixed number of tapers for all frequencies. Spectral derivatives are then estimated and applied in Eq. (5) to generate taper numbers for the next iterate. A new PSD is computed on this basis. The process of refinement of the spectral derivatives and the number of tapers is repeated as many times as desired by the user, although three or four iterations seem to result in a stable result.

We now flesh out some of the details. First, estimating second derivatives of a noisy signal like $\hat{S}_x(f)$ requires some care. Because we require the ratio $S(f)/S''(f)$ in Eq. (8), it is more stable to work with the logarithm $Y(f) = \ln S(f)$ and estimate from the identity

$$\frac{S(f)}{S''(f)} = Y''(f) + Y'(f)^2 \tag{11}$$

rather than finding $S(f)$ and $S''(f)$ separately. Our approach is to fit a degree-two polynomial to the function $Y(f)$ over a small interval about each frequency. With least-squares fitting, the estimates of $Y''(f)$ and $Y'(f)$ become weighted averages of the values of $Y(f)$ in the interval. But what is the proper interval? Here we allow the spectral resolution to set the scale, taking K (as determined in the previous iteration) points on either side of the central frequency.

We come now to the difficulty mentioned at the end of Section 3. If we imagine a frequency interval in which the second derivative S'' passes smoothly through zero, we see from Eq. (8) that the number of tapers increases rapidly without bound. It is found empirically that large values of $|dK_{\text{opt}}/df|$ cause gross distortions in the shape of the estimated spectrum because then the size of the averaging interval fluctuates wildly. The simplification on which the bias in Eq. (4) is based—that the spectrum is well approximated by just three terms of the Taylor series over the averaging interval—must have broken down when one averaging interval entirely covers another. To eliminate this possibility we place constraints on the derivative by requiring

$$|K(f_{j+1}) - K(f_j)| \le 1 \tag{12}$$

which is achieved by running over the K_{opt} series forwards and backwards, enforcing the condition at each frequency index. We find that this simple, *ad hoc* recipe stabilizes the iterative process and leads to quite satisfactory spectra, even though it adds some computational expense. For almost all data-based spectra, however, it has the consequence that the actual number of tapers applied satisfies Eq. (8) only around peaks; elsewhere, much less averaging is done, although, as mentioned earlier, the value of K can still rise to many hundreds (Fig. 5).

5. Application to borehole strainmeter noise

In this section we show an example using `psd` with borehole strainmeter data from the Plate Boundary Observatory (PBO) network. Specifically, we have taken a four-hour sample of high-frequency data (1 Hz sampling) from station B084, located near the San Jacinto fault in southern California. These data are centered in time about the origin of the great M_w9 Tohoku-oki earthquake on 2013/03/11, which occurred offshore of the northeast coast of Japan. We split the record into two approximately equal length segments: one for strain signals prior to any seismic wave arrivals that we term 'pre-seismic' (Fig. 4a); and the other for strains from teleseismic surface waves created by the earthquake (Fig. 4b). The raw records from the four-axis, GTSM-style instrument (see Gladwin, 1984, for details), are in digitizer counts. We have converted these to extensions e_{ij} in a North-East coordinate system using the tidal calibrations of Hodgkinson et al. (2013), and then in combination to form three commonly used measures: areal strain ($e_{\text{NN}} + e_{\text{EE}}$), engineering shear strain ($2e_{\text{NE}}$), and

differential extension ($e_{\text{NN}} - e_{\text{EE}}$). Even though there are more appropriate estimation methods for non-stationary signals, such as the evolutionary spectrum (Priestley, 1981), we isolated three sections in the seismic record which might be considered weakly stationary for comparison; these are labeled A–C in Fig. 4b.

We use `pspectrum` to produce adaptive multitaper PSDs for each component in each section of the seismic record, and for the full pre-seismic record. We remove a second order polynomial from the records to minimize their biasing effects, and perform a four-stage estimation. No other settings are changed from their defaults. Fig. 5 shows how the PSD estimates, the number of tapers, and the uncertainties change with sequential iterations for the pre-seismic data: confidence intervals are smaller, as expected, and after only two iterations the variance is reduced drastically, revealing a spectrum rich with mixed bandwidth features. And these features would be better resolved had we used a much longer record.
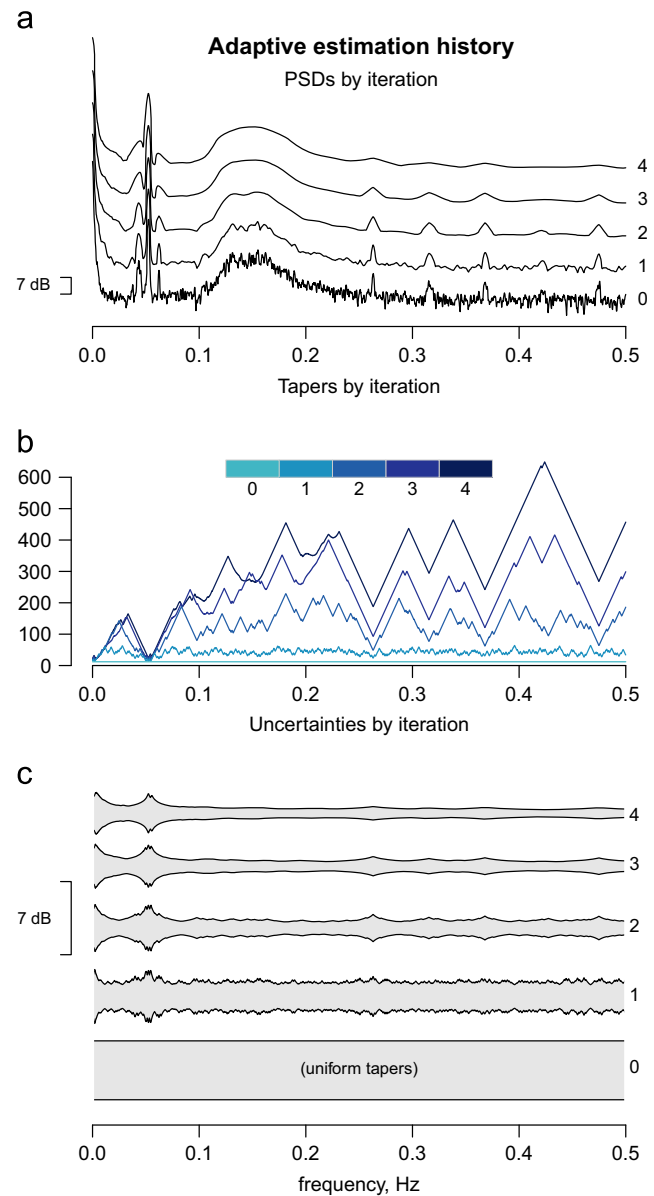

Fig. 5. Adaptive estimation history for pre-seismic areal strains at B084. The quantities shown—for each iteration stage, with zero representing the pilot spectrum—include (a) power spectral density curves, (b) the number of tapers applied, and (c) relative 95% confidence intervals.
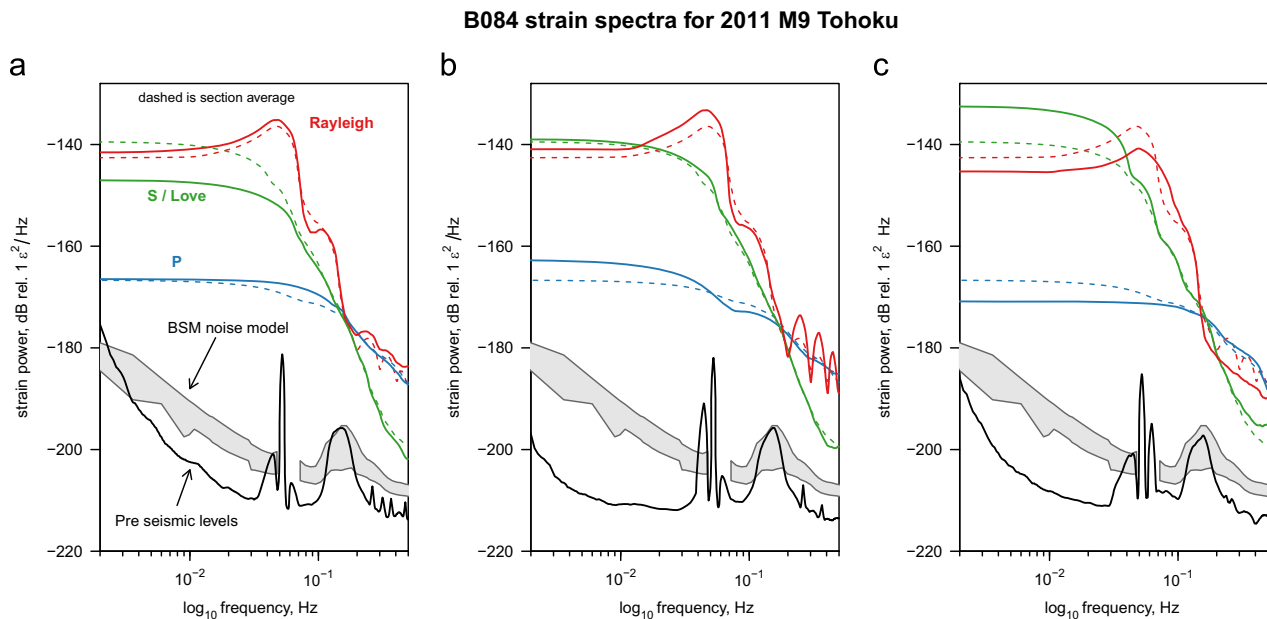
B084 strain spectra for 2011 M9 Tohoku

Fig. 6. Strain spectra at PBO station B084 before, and after the 2011 M_w9 Tohoku-oki earthquake: (a) areal strain, (b) shear strain and (c) differential strain. Curves labeled P, S/Love, and Rayleigh correspond to data sections labeled A–C in Fig. 4(b), respectively; dashed lines show average levels over all components in the data section. Pre-seismic levels are compared to the 10–50th percentile levels from Barbour and Agnew (2011). (For interpretation of the references to color in this figure caption, the reader is referred to the web version of this paper.)

Barbour and Agnew (2011) first documented the statistical variation in noise levels found in data from some PBO strainmeters (including B084) in the 'seismic' frequency band (10^{-3}–10 Hz). They studied the variation in PSD estimates for a year of segmented data, and provide empirical cumulative distribution functions (ecdf) as a function of frequency. The ecdf contours all show a mix of wide and narrow band features, and a 'red' colored spectra commonly found in timeseries having noise with power-law variation (Agnew, 1992). In Fig. 6 we show the spectral estimates for both the pre-seismic and the sectioned seismic records on top of the median and 10th percentiles of the noise model.

The primary wide-band feature seen in the pre-seismic spectra is due to signals from so-called 'dual-frequency' microseisms. Signals in this band arise from interactions between ocean waves and coastal bathymetry, which generate nearly stationary vibrations in the earth's crust. Microseisms are common to every properly functioning seismometer on earth, but have varying amplitudes and dispersion characteristics that depend on local earth structure and distant storm activity (McNamara and Buland, 2004).

The narrow-band features seen in the strain spectra are less interesting from a geophysical perspective, unfortunately, because they are associated with artificial signals created by cycling of the power system (see Instrumental Noise in Barbour and Agnew, 2011). Studies involving surface waves and strain data should thus be scrutinized carefully for contamination by these non-physical signals. Low-power peaks are apparent at much higher frequencies, thanks to the remarkably low noise levels found outside the microseism band during this period of time. The regularly spaced nature of these peaks suggests that some sort of cyclic mechanical device is in operation nearby—a water pump, or an electric generator, perhaps.

See Appendix A for an example using these data and `pspectrum`, and Appendix B for references to alternative PSD estimation tools available for R.

6. Conclusion

We have presented the software package `psd`, an adaptive power spectral density estimation tool using the sine multitapers,

and written for the R programming language. The results are PSD estimates with lower variance and bias relative to commonly used methods (e.g. Welch's). It is also more efficient than non-adaptive multitaper methods (e.g. Slepian tapers) because it requires only one Fourier transform calculation, and needs very little tuning to achieve acceptable results. We used high-frequency borehole strainmeter data to demonstrate how the adaptive multitaper spectrum estimation can resolve a combination of wide- and narrow-bandwidth features in data having a very high dynamic range. In contrast, non-adaptive methods must be adjusted depending on the type of feature to be resolved, and can never produce a single spectrum that combines both types of features.

7. Data and resources

The R programming language is free, and open source under the GNU General Public License (GPL). The source code can be found at http://www.r-project.org, and precompiled installation files exists for a number of common operating systems. The source code and a full reference manual for `psd` is also available under the GPL license, and is hosted by the Comprehensive R Archive Network (CRAN) at http://cran.r-project.org/package=psd. We used R version 3.0.2 and `psd` version 0.4-0 for the examples in this paper. The Tohoku dataset comes from the PBO high-frequency earthquake catalog maintained by K. Hodgkinson. We registered the URL for these data to http://goo.gl/Gx7Ww, and they are included in `psd` (see Appendix A). Websites were last accessed in September, 2013.

Appendix A. Example usage

In this appendix we provide a basic script of R commands demonstrating how to use psd to produce an adaptive PSD estimate for the Tohoku data, specifically the pre-seismic strains (shown in Fig. 4a).

Within the R environment the package can be installed from the CRAN archive with the command

```
install.packages("psd", dependencies = TRUE)
```

which installs all the necessary packages needed to run psd, its examples, tests, and vignettes. (Version updates should be applied using the update.packages function.) Once the necessary packages are installed, the library of functions in psd is loaded with the command

```
library(psd)
```

The Tohoku dataset is included with the package, but not loaded by default. We can load this dataset with the command data, and inspect its contents (stored as an object of the class 'data.frame') with the command str:

```
data(Tohoku)
```

```
str(Tohoku)
```

For this example we want to analyze the pre-seismic portion, so we extract it with the command subset:

```
Dat < −subset(Tohoku, epoch == "preseismic")
```

This data may be visualized in various ways. For example, the commands

```
Areal < −ts(Dat$areal)
```

```
plot(ts.union(Areal, ts(Dat$gamma1),
    ts(Dat$gamma2)))
```

will produce a single figure showing each timeseries in a separate frame, with time in seconds from the beginning of the record.

It is considered good practice to remove a linear model (offset and trend) prior to PSD estimation to prevent potential bias. Various methods exist to do this, but in psd the function prewhiten has this capability:

```
Dat < −prewhiten(Areal, plot = FALSE)
```

and can also be used to remove an auto-regressive model from the data. Next we run pspectrum using default settings for the sampling interval (1 Hz) and the number of iterations (three), which creates a PSD estimate:

```
mtpsd < −pspectrum(Dat$prew_lm, plot = TRUE)
```

Setting the logical argument plot = TRUE will create a figure (in a new window) which compares the final result from pspectrum to a raw periodogram estimate of the same data from spec.pgram in

the built-in stats package library; however, the default is plot = FALSE.

The resulting object, mtpsd, will have the class 'spec' which implies that any available methods may be used. For example, the command

```
plot(mtpsd, log = "dB")
```

accesses the plot.spec method from the stats library, and plots the adaptive power spectral density estimates in units of decibels. Additionally, properties of the spectrum (e.g., uncertainty) may be calculated using the function spectral_properties. For example, the commands

```
sprop < −spectral_properties(mtpsd)
```

calculate various properties of the PSD, stored in object sprop, and the commands

```
Ntap < −sprop$taper/max(sprop$taper)
```

```
plot(Ntap, type = "h",
    ylim = c(0, 2), col = "dark grey")
```

```
lines(sprop$stderr.chi.lower)
```

```
lines(sprop$stderr.chi.upper)
```

overplot 95% confidence intervals of the spectrum on the number of normalized tapers.

Finally, the documentation for psd, or any of its functions may be accessed with the ? command. For example, ?psd opens documentation for the package, and ?pspectrum opens documentation for that function.

Appendix B. Comparisons with other methods in R

In Table 1 we summarize known power spectral density estimation algorithms which are readily available in R (either built in or through extensions). We have excluded any functions (from extensions) which only estimate raw-periodograms. Spectrum normalizations are shown as either 'single' or 'double' for either single- or double-sided spectra, and 'various' if there are other normalizations. The symbol '⁂' indicates that the function has an option for either single or double, but defaults to the normalization shown.

Comparisons between our method and others shown in Table 1 can be found in the vignette named "psd_overview", which can be accessed within the R environment with the command vignette. For example, the command

```
vignette("psd_overview", package = "psd")
```

will open the vignette as a pdf document. See ?vignette for more details.

Table 1
Power spectral density estimators in R.

Function	Package	Sine m.t.?[a]	Adaptive?	Norm.[b]	Reference
bspec	bspec	No	No	Single*	Roever (2013)
mtapspec	RSEIS	Yes	No	Various	Lees (2013)
pspectrum	psd	Yes	Yes	Single	This paper
spectrum	stats	No	No	Double	R Core Team (2013)
spec.mtm	multitaper	Yes	Yes	Double	Rahim and Burr (2012)
SDF	sapa	Yes	No	Single*	Constantine and Percival (2012)

* denotes the default, but has an option for either single or double.
  [a] Sine multitaper method.
  [b] Spectrum normalization. Can be either single-sided, double-sided, or a variety.

References

Agnew, D.C., 1992. The time-domain behavior of power-law noises. Geophysical Research Letters 19 (4), 333–336.

Barbour, A.J., Agnew, D.C., 2011. Noise levels on Plate Boundary Observatory borehole strainmeters in Southern California. Bulletin of the Seismological Society of America 101 (5), 2453–2466, http://dx.doi.org/10.1785/0120110062.

Constantine, W., Percival, D., 2012. sapa: Spectral Analysis for Physical Applications, R package version 1.1-0, http://cran.r-project.org/package=sapa.

Cowpertwait, P.S.P., Metcalfe, A.V., 2009. Introductory Time Series with R, first ed. Springer Publishing Company, Incorporated.

Gladwin, M.T., 1984. High precision multicomponent borehole deformation monitoring. Review of Scientific Instruments 55 (12), 2011.

Hodgkinson, K., Langbein, J., Henderson, B., Mencin, D., Borsa, A., 2013. Tidal calibration of Plate Boundary Observatory borehole strainmeters. Journal of Geophysical Research 118 (1), 447–458, http://dx.doi.org/10.1029/2012JB009651.

Lees, J.M., 2013. RSEIS: Seismic Time Series Analysis Tools. R package version 3.2-1, http://cran.r-project.org/package=RSEIS.

McNamara, D.E., Buland, R.P., 2004. Ambient noise levels in the Continental United States. Bulletin of the Seismological Society of America 94 (4), 1517–1527.

Percival, D., Walden, A., 1993. Spectral Analysis for Physical Applications. Cambridge University Press.

Priestley, M.B., 1981. Spectral Analysis and Time Series. Academic, Orlando, FL 890 pp.

Prieto, G.A., Parker, R.L., Thomson, D.J., Vernon, F.L., Graham, R.L., 2007. Reducing the bias of multitaper spectrum estimates. Geophysical Journal International 171, 1269–1281.

R Core Team, 2013. R: A Language and Environment for Statistical Computing. R Foundation for Statistical Computing, Vienna, Austria, ISBN 3-900051-07-0.

Rahim, K., Burr, W., 2012. multitaper: Multitaper Spectral Analysis. R package version 1-0, http://cran.r-project.org/package=multitaper.

Riedel, K., Sidorenko, A., 1995. Minimum bias multiple taper spectral estimation. IEEE Transactions on Signal Processing 43 (1), 188–195, http://dx.doi.org/10.1109/78.365298.

Roever, C., 2013. bspec: Bayesian spectral inference. R package version 1.4, http://cran.r-project.org/package=bspec.

Slepian, D., 1961. Prolate spheroidal wave functions, Fourier analysis, and uncertainty—I. Bell System Technical Journal 40, 43–64.

Thomson, D.J., 1982. Spectrum estimation and harmonic analysis. In: Proceedings of the IEEE, vol. 70. Bell Labs, pp. 1055–1096.

Welch, P., 1967. The use of fast Fourier transform for the estimation of power spectra: a method based on time averaging over short, modified periodograms. IEEE Transactions on Audio and Electroacoustics 15 (2), 70–73, http://dx.doi.org/10.1109/TAU.1967.1161901.